



US 20180055425A1

(19) **United States**

(12) **Patent Application Publication**
Xu

(10) **Pub. No.: US 2018/0055425 A1**
(43) **Pub. Date: Mar. 1, 2018**

(54) **METHOD AND SYSTEM FOR
NON-INVASIVE OPTICAL BLOOD GLUCOSE
DETECTION UTILIZING SPECTRAL DATA
ANALYSIS**

(52) **U.S. Cl.**
CPC *A61B 5/14532* (2013.01); *A61B 5/1455*
(2013.01); *A61B 2562/0238* (2013.01); *A61B*
5/7225 (2013.01); *A61B 5/6826* (2013.01);
A61B 5/6838 (2013.01)

(71) Applicant: **St. Louis Medical Devices, Inc.**,
Sunnyvale, CA (US)

(72) Inventor: **Zhi Xu**, St. Louis, MO (US)

(57) **ABSTRACT**

(21) Appl. No.: **15/806,242**

(22) Filed: **Nov. 7, 2017**

Related U.S. Application Data

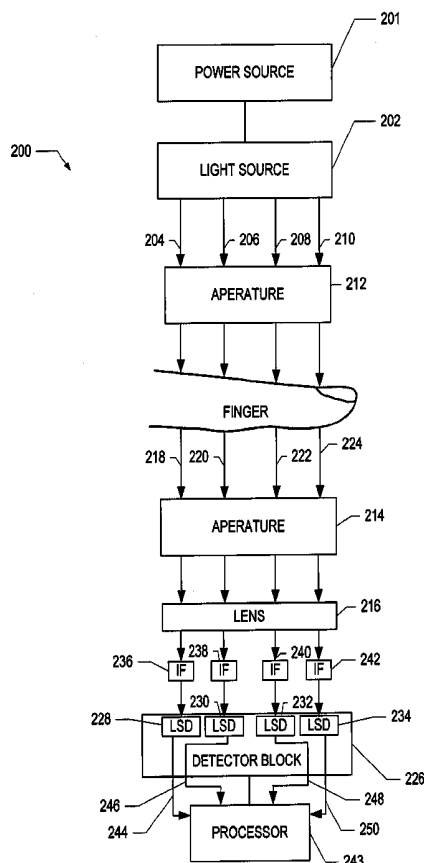
(60) Continuation of application No. 13/610,387, filed on Sep. 11, 2012, now Pat. No. 9,814,415, which is a division of application No. 12/425,535, filed on Apr. 17, 2009, now Pat. No. 8,340,738.

(60) Provisional application No. 61/055,303, filed on May 22, 2008, provisional application No. 61/089,152, filed on Aug. 15, 2008.

Publication Classification

(51) **Int. Cl.**
A61B 5/145 (2006.01)
A61B 5/1455 (2006.01)
A61B 5/00 (2006.01)

Systems and methods are disclosed for non-invasively measuring blood glucose levels in a biological sample based on spectral data. This includes at least one light source configured to strike a target area of a sample, at least one light detector, which includes a preamplifier having a feedback resistor, positioned to receive light from the at least one light source and to generate an output signal, having a time dependent current, which is indicative of the power of light detected, and a processor configured to receive the output signal from the at least one light detector and based on the received output signal, calculate the attenuation attributable to blood in a sample present in the target area and eliminate effect of uncertainty caused by temperature dependent detector response of the at least one light detector, and based on the calculated attenuation, determine a blood glucose level associated with a sample.



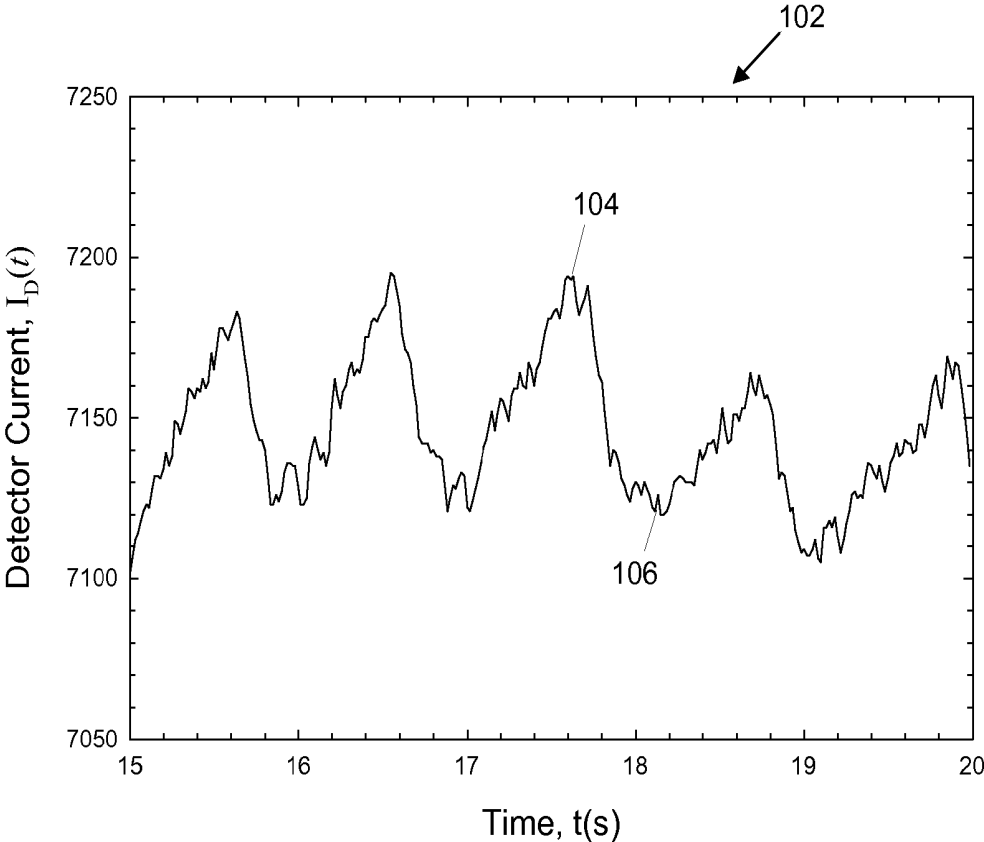
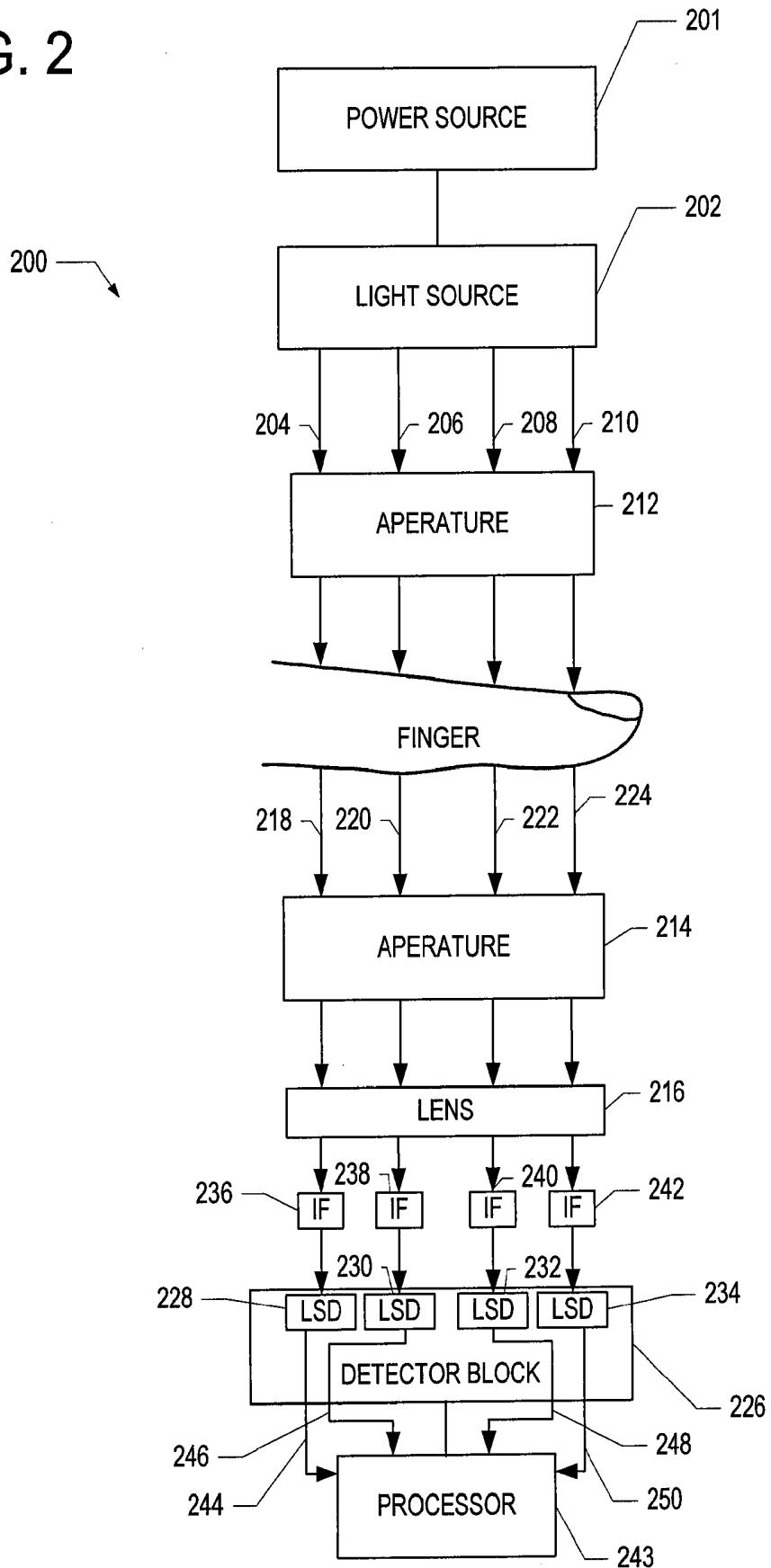


FIG. 1

FIG. 2



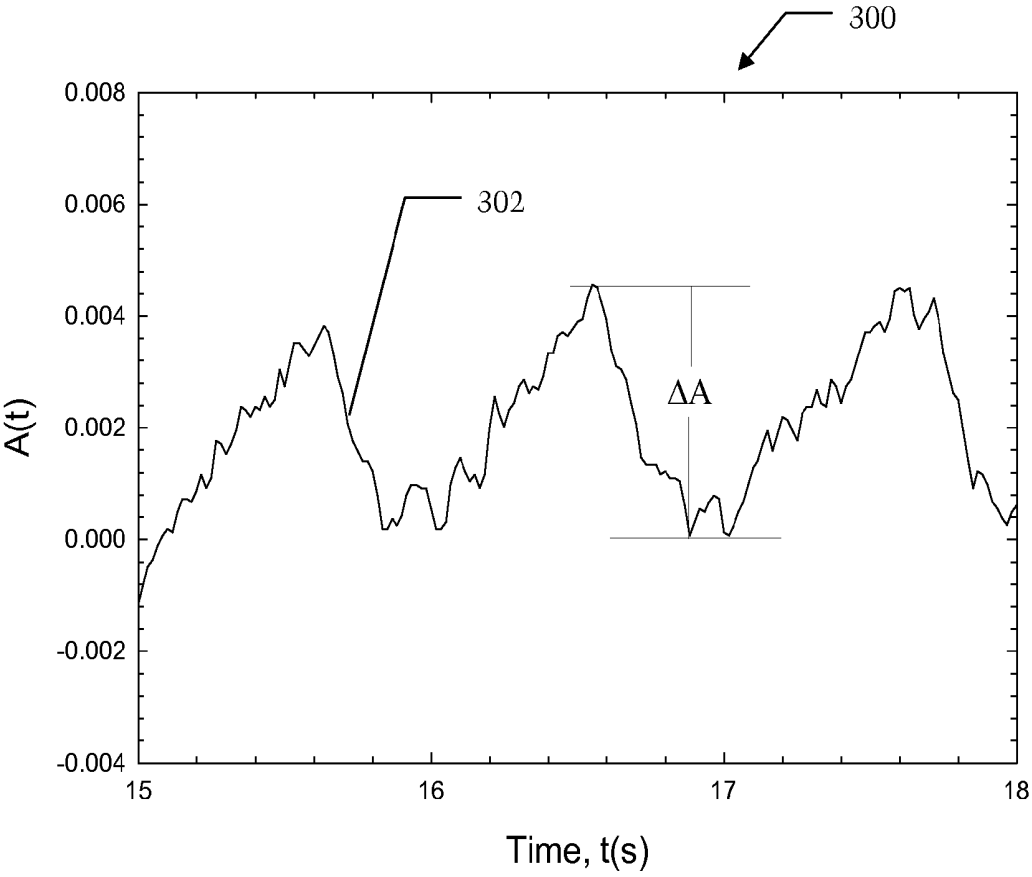


FIG. 3

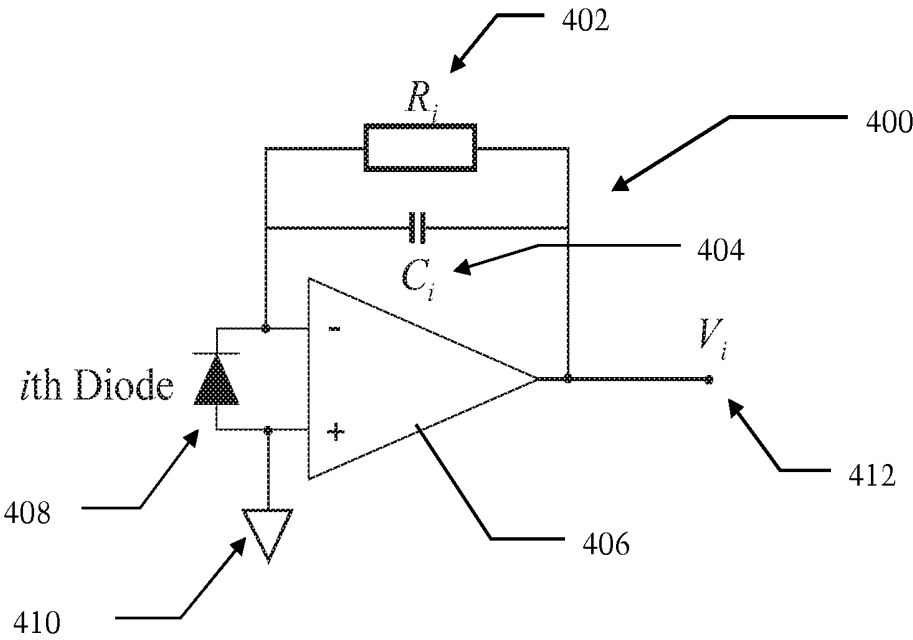


FIG. 4

**METHOD AND SYSTEM FOR
NON-INVASIVE OPTICAL BLOOD GLUCOSE
DETECTION UTILIZING SPECTRAL DATA
ANALYSIS**

CROSS-REFERENCE TO RELATED
APPLICATION

[0001] This application is a divisional of prior U.S. patent application Ser. No. 12/425,535, filed Apr. 17, 2009, which is hereby incorporated herein by reference in its entirety, and also claims priority to U.S. Provisional Patent Application Ser. No. 61/055,303, filed on May 22, 2008, the disclosure of which is incorporated herein by reference, and also claims priority to U.S. Provisional Patent Application Ser. No. 61/089,152, filed on Aug. 15, 2008, the disclosure of which is incorporated herein by reference.

BACKGROUND OF THE INVENTION

[0002] Diabetes is a chronic disease that, when not controlled, over time leads to serious damage to many of the body's systems, including the nerves, blood vessels, eyes, kidneys and heart. The National Institute of Diabetes and Digestive and Kidney Diseases (NIDDK) estimates that 23.6 million people, or 7.8 percent of the population in the United States, had diabetes in 2007. Globally, the World Health Organization (WHO) estimates that more than 180 million people have diabetes, a number they expect to increase to 366 million by 2030, with 30.3 million in the United States. According to the WHO, an estimated 1.1 million people died from diabetes in 2005. They project that diabetes deaths will increase by more than 50% between 2006 and 2015 overall and by more than 80% in upper-middle income countries.

[0003] The economic burden from diabetes for individuals and society as a whole is substantial. According to the American Diabetes Association, the total annual economic cost of diabetes was estimated to be \$174 billion in the United States in 2007. This is an increase of \$42 billion since 2002. This 32% increase means the dollar amount has risen over \$8 billion more each year.

[0004] A vital element of diabetes management is the self-monitoring of blood glucose (SMBG) concentration by diabetics in the home environment. By testing blood glucose levels often, diabetics can better manage medication, diet, and exercise to maintain control and prevent the long-term negative health outcomes. In fact, the Diabetes Control and Complications Trial (DCCT), which followed 1,441 diabetics for several years, showed that those following an intensive-control program with multiple blood sugar tests each day, as compared with the standard-treatment group, had only one-fourth as many people develop diabetic eye disease, half as many develop kidney disease, one-third as many develop nerve disease, and far fewer people who already had early forms of these three complications got worse.

[0005] However, current monitoring techniques discourage regular use due to the inconvenient and painful nature of drawing blood through the skin prior to analysis, which causes many diabetics to not be as diligent as they should be for good blood glucose control. As a result, non-invasive measurement of glucose concentration is a desirable and beneficial development for the management of diabetes. A non-invasive monitor will make testing multiple times each day pain-free and more palatable for children with diabetes.

According to a study published in 2005 (J. Wagner, C. Malchoff, and G. Abbott, *Diabetes Technology & Therapeutics*, 7(4) 2005, 612-619), people with diabetes would perform SMBG more frequently and have improved quality of life with a non-invasive blood glucose monitoring device.

[0006] There exist a number of non-invasive approaches for blood glucose determination. One technique of non-invasive blood chemical detection involves collecting and analyzing light spectra data.

[0007] Extracting information about blood characteristics, such as glucose concentration from spectral or other data obtained from spectroscopy, is a complex problem due to the presence of components (e.g., skin, fat, muscle, bone, interstitial fluid) other than blood in the area that is being sensed. Such other components can influence these signals in such a way as to alter the reading. In particular, the resulting signal may be much larger in magnitude than the portion of the signal that corresponds to blood, and therefore limits the ability to accurately extract blood characteristics information.

[0008] The present invention is directed to overcoming one or more of the problems set forth above.

SUMMARY OF INVENTION

[0009] In an aspect of the present invention, a system for detecting glucose in a biological sample is disclosed. This system includes at least one light source configured to strike a target area of a sample, at least one light detector, which includes a preamplifier having a feedback resistor, positioned to receive light from the at least one light source and to generate an output signal, having a time dependent current, which is indicative of the power of light detected, and a processor configured to receive the output signal from the at least one light detector and based on the received output signal, calculate the attenuation attributable to blood in a sample present in the target area and eliminate effect of uncertainty caused by temperature dependent detector response of the at least one light detector, and based on the calculated attenuation, determine a blood glucose level associated with a sample present in the target area.

[0010] In yet another aspect of the present invention, a method for detecting glucose in a biological sample is disclosed. The method includes utilizing at least one light source configured to strike a target area of a sample utilizing at least one light detector, which includes a preamplifier having a feedback resistor, positioned to receive light from the at least one light source and generating an output signal, having a time dependent current, which is indicative of the power of light detected, and utilizing a processor that receives the output signal from the at least one light detector and based on the received output signal, calculating the attenuation attributable to blood in a sample present in the target area and eliminating effect of uncertainty caused by temperature dependent detector response of the at least one light detector, and based on the calculated attenuation, determining a blood glucose level associated with a sample present in the target area.

[0011] These are merely some of the innumerable aspects of the present invention and should not be deemed an all-inclusive listing of the innumerable aspects associated with the present invention.

BRIEF DESCRIPTION OF THE DRAWINGS

[0012] For a better understanding of the present invention, reference may be made to accompanying drawings, in which:

[0013] FIG. 1 illustrates a plot of a pulse wave corresponding to light absorption of arterial blood, according to exemplary embodiments;

[0014] FIG. 2 illustrates an exemplary system for obtaining spectral data;

[0015] FIG. 3 illustrates a plot of $A(t)$, calculated according to Equation (9) using data in FIG. 1; and

[0016] FIG. 4 is a basic illustrative schematic of a preamplifier circuit that converts photocurrent into voltage prior to digitization.

DETAILED DESCRIPTION OF THE INVENTION

[0017] In the following detailed description, numerous exemplary specific details are set forth in order to provide a thorough understanding of the invention. However, it will be understood by those skilled in the art that the present invention may be practiced without these specific details, or with various modifications of the details. In other instances, well known methods, procedures, and components have not been described in detail so as not to obscure the present invention.

[0018] Optical spectroscopy can be used to determine the amount of light absorbed and scattered, i.e., attenuated, by a biological sample such as a human finger. By measuring the amount of light absorbed by the sample, it is possible to determine glucose, cholesterol, and hemoglobin levels of a subject non-invasively. Fingertip measurements are usually preferred because of the large concentration of capillaries in the fingertip and because of the conversion of arterial blood into venous blood that occurs in the fingertip. However, the techniques of the present invention are not limited to use with a fingertip. For example, the biological sample could be a human earlobe.

[0019] When light is transmitted through a biological sample, such as a human finger, the light is attenuated by various components of the finger including skin, muscle, bone, fat, interstitial fluid and blood. It has been observed, however, that light attenuation by a human finger exhibits a small cyclic pattern that corresponds to a heartbeat. It is believed that this cyclic pattern will be present in measurements of many other human body parts, the earlobe being one of many examples.

[0020] FIG. 1 depicts a plot 102 of a detector photocurrent, $I_D(t)$, that corresponds to the power of light received by a detector after the light has passed through a subject's finger. As can be seen, the detector photocurrent exhibits a cyclic pattern. This cyclic pattern is due to the subject's heartbeat, which cyclically increases and decreases the quantity of blood in the subject's capillaries (or other structures). Although the magnitude of the cyclic pattern is small in comparison to the total photocurrent generated by the detector, considerable information can be extracted from the cyclic pattern of the plot 102. For example, assuming that the person's heart rate is sixty beats per minute, the time between the start of any pulse beat and the end of that pulse beat is one second. During this one-second period, the photocurrent will have a maximum or peak reading 104 and minimum or valley reading 106. The peak reading 104 of the

plot corresponds to when there is a minimum amount of blood in the capillaries, and the valley reading 106 corresponds to when there is a maximum amount of blood in the capillaries. By using information provided by the peak and valley of the cyclic plot, the optical absorption and scattering by major finger constituents that are not in the capillaries, such as skin, fat, bones, muscle and interstitial fluids, are excluded. These major constituents that are not in the capillaries are excluded because they are not likely to change during the time interval of one heartbeat. In other words, the light that is absorbed and scattered, i.e., attenuated, by the blood can be detected based on the peaks and valleys of the plot 102.

[0021] Assuming that the peak of the cyclic photocurrent generated by the light-sensing device is I_P , the adjacent valley of the cyclic photocurrent is I_V , and the photocurrent generated by the light-sensing device without a human finger is I_0 , the transmittances corresponding to the peak and valley photocurrents can be defined as:

$$T_V = \frac{I_V}{I_0} \quad (1)$$

and

$$T_P = \frac{I_P}{I_0} \quad (2)$$

[0022] The corresponding peak and valley absorbance are:

$$A_V = \log(T_V) \quad (3)$$

and

$$A_P = \log(T_P) \quad (4)$$

[0023] The difference between A_V and A_P represents the light absorption and scattering by the blood in the finger, excluding non-blood constituents:

$$\Delta A = A_V - A_P = \log\left(\frac{I_P}{I_V}\right) \quad (5)$$

[0024] As can be seen in the algorithm shown in Equation (5), ΔA does not depend on I_0 . Thus, calculating ΔA does not require a determination of the current generated by the light-sensing device without a sample. Monitoring the photocurrent corresponding to light power transmitted through a sample is sufficient to calculate ΔA .

[0025] FIG. 2 depicts a simplified block diagram of an exemplary apparatus for use in an exemplary embodiment. Optical measurement system, which is generally indicated by numeral 200, uses the "pulsatile" concept for determining an amount of light absorbed and scattered solely by the blood in a sample (a human finger in this exemplary embodiment). A power source 201, such as a battery, provides power to a light source 202 that generates a plurality of light beams 204, 206, 208, 210 that are directed toward the top of the finger of a subject. In an exemplary embodiment, each of the light beams 204, 206, 208, 210 have the same wavelength or a different wavelength range, typically within 800 nm to 1600 nm. Although the optical measurement system 200 is described herein as generating four (4) light beams,

it is contemplated that the light source 202 can be altered to generate fewer light beams or additional light beams in other embodiments.

[0026] A first aperture 212 ensures that the light beams 204, 206, 208, 210 strike a target area of the finger. A second aperture 214 ensures that the portion of the light beams that are transmitted through the finger strike a lens 216. Light beams 204, 206, 208, 210 are attenuated by the finger and components of the optical measurement system 200, and, thus, attenuated light beams 218, 220, 222, 224 are emitted from the finger. The attenuated light beams 218, 220, 222, 224 strike the lens 216, and the lens 216 collects the attenuated light beams 218, 220, 222, 224 so that they impinge more efficiently on a detector block 226.

[0027] The detector block 226 is positioned directly under the lens 216 and comprises a plurality of light-sensing devices (LSD) 228, 230, 232, 234 such as an array of photodiodes. According to one aspect of the optical measurement system 200, each of the light-sensing devices 228, 230, 232, 234 detects a specific wavelength of light as defined by corresponding interference filters (IF) 236, 238, 240, 242, respectively. The interference filter transmits one or more spectral bands or lines of light, and blocks others.

[0028] Each of the light-sensing devices 228, 230, 232, 234 generates a corresponding photocurrent signal that is proportional to the power of the light received by the particular light sensing device. The photocurrent signal generated by the photodiode can be converted to another form of signal, such as an analog voltage signal or a digital signal. A processor 243 is coupled to the detector block 226 and is configured to calculate the change of photocurrent signals 244, 246, 248, 250.

[0029] According to one aspect, the processor 243 executes an algorithm such as shown in the Equation (5) to calculate the change in the light absorption (AA) solely caused by the blood in the finger. Thereafter, this quantitative calculation of light absorption of the blood can be used to determine a characteristic of the blood. For example, by comparing the calculated light absorption value to predetermined values corresponding to different glucose levels stored in a memory (not shown), a blood-glucose level of the subject can be determined.

[0030] A difficulty associated with the finger based pulsatile detection methodology is low signal-to-noise (S/N) ratio, because the amplitude of cyclic pattern (i.e., the difference between peak and valley) is typically 1%-2% of the total photocurrent generated by the light power transmitted through the finger. To obtain a S/N ratio of 100:1 in the determination of AA, the baseline noise of the device being used to measure the light absorption by the finger should not be larger than 3.0×10^{-5} in absorbance (peak to peak), within a 10 Hz bandwidth.

[0031] However, a 3.0×10^{-5} absorbance (peak to peak) baseline noise level within a 10 Hz bandwidth is difficult to obtain with the low light power levels that are used by some battery-powered hand held non-invasive blood chemical measurement devices. One solution involves data averaging. To increase the S/N ratio, the averaged value of ΔA , as defined by the Equation below, is used in further calculation to extract blood glucose concentration:

$$\overline{\Delta A} = \sum_{j=1}^M \Delta A_j \quad (6)$$

[0032] In Equation (6), M is the number of heartbeats during the time interval of the pulsatile measurement. However, this approach requires long data acquisition time, due to the fact that the rate of heartbeat is in the order of one per second. For example, 25 seconds would be needed for increasing the S/N ratio by a factor of five, and 100 seconds would be needed for increasing the S/N ratio by a factor of ten. In comparison, current commercial blood drawing glucose meters can determine blood glucose level within 5 seconds. Furthermore, long detection time will significantly increase measurement errors due to finger movement, light power drift, device temperature change, etc. Thus, there is a need for new techniques to measure blood glucose levels quickly and accurately.

Improving S/N Ratio by Standard Deviation

[0033] The time dependent detector photocurrent output, $I_D(t)$, shown in FIG. 1 can be expressed as the sum of a small time dependent cyclic photocurrent $\Delta I(t)$, corresponding to the heartbeat, a noise current $n(t)$, and a constant baseline photocurrent I_B :

$$I_D(t) = I_B + \Delta I(t) + n(t) \quad (7)$$

[0034] The above Equation can be re-arranged as:

$$\frac{I_D(t)}{I_B} = 1 + \frac{\Delta I(t) + n(t)}{I_B} \quad (8)$$

[0035] Applying common logarithm to both side of the Equation (8), one obtains:

$$A(t) = \log \left[\frac{I_D(t)}{I_B} \right] = \log \left(1 + \frac{\Delta I(t) + n(t)}{I_B} \right) \quad (9)$$

[0036] FIG. 3, which is generally indicated by numeral 300, shows a typical A(t) plot 302, calculated according to Equation (9) using data in FIG. 1. For a pulse function A(t) shown in FIG. 3, the following key relationship exists during the time interval of one heartbeat:

$$\sigma[A(t)] = k \Delta A \quad (10)$$

in which $\sigma[A(t)]$ is the Standard Deviation of A(t), and k is a proportional constant.

[0037] Considering the fact that I_B is a constant and $\sigma^2(\log I_B) = 0$, one obtains:

$$\sigma[A(t)] = \sigma[\log I_D(t)] \quad (12)$$

[0038] Therefore, the peak-to-valley height of the A(t) plot during the time interval of one heartbeat can be obtained directly from the standard deviation of the logarithm of $I_D(t)$:

$$\Delta A = \frac{\sigma[A(t)]}{k} = \frac{\sigma[\log I_D(t)]}{k} \quad (13)$$

A major advantage of Equation (13) is that high S/N ratio can be achieved within short data acquisition time (approximately one second), as explained below.

[0039] In a finger based pulsatile measurement depicted by FIG. 2, the value of the sum, $\Delta I(t)+n(t)$ is typically less than 2% of the large constant baseline photocurrent I_B . Therefore, Equation (9) can be approximated as:

$$A(t) = \log\left[\frac{I_D(t)}{I_B}\right] \approx \frac{1}{\ln 10} \frac{\Delta I(t) + n(t)}{I_B} \quad (14)$$

[0040] Similarly, the standard deviation of $A(t)$ can be approximated as:

$$\sigma[A(t)] \approx \frac{1}{\ln 10} \frac{\sqrt{\sigma^2[\Delta I(t)] + \sigma^2[n(t)]}}{I_B} \quad (15)$$

[0041] Equation (15) demonstrates great noise reduction power of Equation (13). For example, for a relatively high baseline noise with the ratio

$$\rho = \frac{\sigma[n(t)]}{\sigma[\log \Delta I(t)]} = 0.1 \text{ (or 10\%)},$$

the contribution to $\sigma[A(t)]$ from the baseline noise $n(t)$ is estimated to be less than 0.005 (or 0.5%), corresponding to an increase in S/N ratio by a factor of 20 without increasing detection time. As such, dramatic noise reduction can be obtained without increasing the data acquisition time, and a finger based pulsatile measurement can be completed within the time interval of one heartbeat (which is approximately one second), and the requirement for the S/N ratio of 100 to 1 in determination of AA can be satisfied using an optical system with a baseline noise of about 6.0×10^{-4} absorbance (peak to peak) within a 10 Hz bandwidth. It should be pointed out that when the baseline noise of an optical system is dominated by shot noise due to low light illumination power, a noise reduction by a factor of 20 equals an increasing in light illumination power by a factor of $20^2=400$.

[0042] This ability of obtaining higher S/N ratio within the very short data acquisition time, e.g., less than one second, will significantly reduce detection error caused by factors such as finger movement, temperature change, and light power drift during the measurement, and therefore dramatically improve the accuracy and reproducibility of the pulsatile detection methodology.

[0043] Furthermore, the value of k does not change with wavelength, because transmitted lights at all wavelengths have identical pulse shape due to the heartbeat. As a result, the constant k will be cancelled in data normalization discussed in next section, and $\sigma[\log I_D(t)]$ will be used in further regression analysis to establish correlation between the optical measurement and blood glucose level. This will greatly simplify the data analysis process since $\sigma[\log I_D(t)]$ involves only two standard math functions available in most popular spreadsheet programs such as Microsoft EXCEL®. EXCEL® is a federally registered trademark of Microsoft

Corporation, having a place of business at One Microsoft Way, Redmond, Wash. 98052-6399.

Normalization

[0044] At each wavelength λ_i , the absorption $\Delta A(\lambda_i)$ is linked to the increase of amount of blood (ΔB) in the optical sensing area of the fingertip due to the heartbeat by the following Equation:

$$\Delta A(\lambda_i) = \epsilon(C, \lambda_i, T) \Delta B \quad (16)$$

in which $\epsilon(C, \lambda_i, T)$ is the absorption/scattering coefficient of blood at wavelength λ_i , finger temperature T , and blood glucose concentration C . It is well understood that the variable ΔB differs from person to person, and may even change from day to day for the same person.

[0045] The uncertainty from the variable ΔB can be cancelled by introducing the normalization factor $Q_i(C, T)$ at each wavelength λ_i , as defined by the Equation below:

$$Q_i(C, T) = \frac{\Delta A(\lambda_i)}{\sum_{i=1}^N \Delta A(\lambda_i)} = \frac{\epsilon(C, \lambda_i, T)}{\sum_{i=1}^N \epsilon(C, \lambda_i, T)}, \quad (17)$$

in which N is total number of wavelength employed. Preferably, N typically ranges from twenty to thirty.

[0046] Based on Equations (13) and (17), $Q_i(C, T)$ is linked to the detector photocurrent at each wavelength λ_i , $I_D(\lambda_i, t)$, by the following Equation:

$$Q_i(C, T) = \frac{\Delta A(\lambda_i)}{\sum_{i=1}^N \Delta A(\lambda_i)} = \frac{\sigma[\log I_D(\lambda_i, t)]/k}{\sum_{i=1}^N \sigma[\log I_D(\lambda_i, t)]/k} = \frac{\sigma[\log I_D(\lambda_i, t)]}{\sum_{i=1}^N \sigma[\log I_D(\lambda_i, t)]}, \quad (18)$$

[0047] As shown by Equation (18), the constant k is cancelled and $\sigma[\log I_D(t)]$ will be used in further regression analysis to establish correlation between the optical measurement and blood glucose level. This is possible because data are taken simultaneously from all detection channels.

[0048] A correlation between optical measurement and blood glucose concentration can be established according to the following Equation:

$$C_{optical} = \sum_{i=1}^N a_i(T) Q_i(C, T) \quad (19)$$

[0049] in which $C_{optical}$ is the blood glucose concentration predicted by the optical measurement, $Q_i(C, T)$ is defined by Equations (17) and (18), and $a_i(T)$ is the temperature dependent regression coefficient corresponding to wavelength λ_i . The values of $a_i(T)$ can be extracted using proper statistics methods such as Partial Least Squares (PLS) regression.

[0050] Equation (19) represents ideal cases when large number of calibrations can be made at different finger temperatures. In reality, frequently only a limited number of calibrations can be made (e.g., 15 to 20), and each may be taken at a different finger temperature. Under this condition, the finger temperature can be treated as an independent variable, and the above Equation can be approximated as:

$$C_{optical} = \sum_{i=1}^N b_i Q_i(C, T) + \eta T \quad (20)$$

in which b_i is the temperature independent regression coefficient corresponding to wavelength λ_i , and η is the regression coefficient for the finger temperature. The values of b_i and that of η can be extracted using proper statistics methods such as Partial Least Squares (PLS) regression.

Ratio Methodology

[0051] Alternatively, the uncertainty from the variable ΔB can be cancelled by introducing a ratio factor Y_{ij} at wavelength λ_i :

$$Y_{ij}(C, T) = \frac{\Delta A(\lambda_i)}{\Delta A(\lambda_j)} = \frac{\varepsilon(C, \lambda_i, T)}{\varepsilon(C, \lambda_j, T)} = \frac{\sigma[\log I_D(\lambda_i, t)]}{\sigma[\log I_D(\lambda_j, t)]} \quad (21)$$

in which j can be any number from 1 to N , assuming that the device collects signal at all N wavelengths.

[0052] Similar to the normalization algorithm discussed before, a correlation between optical measurement and blood glucose level can be established according to the following Equation:

$$C_{optical} = \sum_{i \neq j}^N f_i(T) Y_{ij}(C, T) \quad (22)$$

in which $C_{optical}$ is the blood glucose concentration predicted by the optical measurement, $Y_{ij}(C, T)$ is defined by Equation (21), and $f_i(T)$ is the temperature dependent regression coefficient corresponding to wavelength λ_i . The value of $f_i(T)$ can be obtained using statistics methods such as Partial Least Squares (PLS) regression.

[0053] Equation (22) represents ideal cases when large number of calibration can be made at different finger temperatures. In reality, frequently only limited number of calibration can be made (e.g., 15 to 20), and each may be taken at a different finger temperature. Under this condition, the finger temperature can be treated as an independent variable, and the above Equation can be approximated as:

$$C_{optical} = \sum_{i \neq j}^N h_i Y_{ij}(C, T) + \beta T \quad (23)$$

in which h_i is the temperature independent regression coefficient corresponding to wavelength λ_i , and β is the regression coefficient for the finger temperature. The values of h_i and that of β can be extracted using proper statistics methods such as Partial Least Squares (PLS) regression.

Elimination of the Effect of Temperature Dependent Device Response

[0054] It is well understood that the detector sensitivity of a silicon photodiode detector is a function of wavelength and temperature. For the device configuration shown in FIG. 2,

which is generally indicated by numeral **200**, the light power received by i th silicon diode detector, corresponding to wavelength λ_i , is converted into a photocurrent according to the following Equation:

$$I_D(\lambda_i, t) = P(\lambda_i, t) S_0(\lambda_i) [1 + \gamma(\lambda_i)(T_{Di}(t) - 25^\circ \text{ C.})] \quad (24)$$

[0055] In the above Equation (24), $P(\lambda_i, t)$ is the light power received by the detector, $S_0(\lambda_i)$ is the photosensitivity of the detector at wavelength λ_i and 25° C. , $\gamma(\lambda_i)$ is the temperature coefficient of the photosensitivity at wavelength λ_i , and $T_{Di}(t)$ is the temperature of i th photodiode detector. The temperature coefficient $\gamma(\lambda_i)$ varies with the wavelength. For example, for Hamamatsu S1337 series photodiode detectors, $\gamma(\lambda_i)$ ranges from near zero at 900 nm to over $1.0\%/^\circ \text{ C.}$ at 1100 nm. This imposes a potential problem for the device configuration shown in FIG. 2, because it is very difficult to keep temperature of each individual diode detector constant in a handheld device used by a person with diabetes under a normal household/office environment.

[0056] This uncertainty due to the detector temperature $T_{Di}(t)$ can be eliminated using the algorithm shown by Equations (12) and (13). Applying common logarithm on both sides of the Equation (24), one obtains:

$$\log I_D(\lambda_i, t) = \log P(\lambda_i, t) + \log S_0(\lambda_i) + \log [1 + \gamma(\lambda_i)(T_{Di}(t) - 25^\circ \text{ C.})] \quad (25)$$

[0057] Considering the fact that $S_0(\lambda_i)$ is a constant and that detector temperature $T_{Di}(t)$ remains almost constant during the very short data acquisition time interval of approximately one second, one obtains:

$$\sigma[\log I_D(\lambda_i, t)] = \sigma[\log P(\lambda_i, t)] \quad (26)$$

As such, the uncertainty caused by detector temperature $T_{Di}(t)$ is eliminated by the use of this standard deviation methodology.

Voltage Detection Mode

[0058] In the device configuration shown in FIG. 2, the photocurrent of i th photodiode detector $I_D(\lambda_i, t)$ is typically converted into a voltage using a preamplifier before digitization. FIG. 4 shows the schematic circuit diagram of a typical preamplifier, which is generally indicated by numeral **400**.

[0059] The output voltage **412** of i th preamplifier **400**, in coupling with i th photodiode detector **408**, can be expressed as:

$$V_i(t) = R_i I_D(\lambda_i, t) R_{0i} [1 + \chi_i(T_{Ri}(t) - 25^\circ \text{ C.})] I_D(\lambda_i, t) \quad (27)$$

[0060] In the above Equation (27), R_{0i} is the resistance value of feedback resistor **402** for i th preamplifier at 25° C. , χ_i is the temperature coefficient of the resistor, and $T_{Ri}(t)$ is the temperature of the resistor. Applying common logarithm to both side of the Equation (27), one obtains:

$$\log V_i(t) = \log R_{0i} + \log [1 + \chi_i(T_{Ri}(t) - 25^\circ \text{ C.})] + \log I_D(\lambda_i, t) \quad (28)$$

[0061] Considering the fact that R_{0i} is a constant and that the resistor temperature $T_{Ri}(t)$ does not change during the very short data acquisition time interval of approximately one second, one obtains:

$$\sigma[\log V_i(t)] = \sigma[\log I_D(\lambda_i, t)] \quad (29)$$

[0062] Substituting Equation (26) into Equation (29), one obtains:

$$\sigma[\log V_i(t)] = \sigma[\log P(\lambda_i, t)] \quad (30)$$

As such, the uncertainty caused by resistor temperature $T_R(t)$ is eliminated.

[0063] Under the voltage detection mode, the normalization factor in Equation (18) can be expressed as:

$$Q_i(C, T) = \frac{\sigma[\log V_i(t)]}{\sum_{i=1}^N \sigma[\log V_i(t)]} \quad (31)$$

[0064] The mathematic correlation between optical measurement and blood glucose concentration can then be established according to Equation (19) or Equation (20), under corresponding calibration conditions.

[0065] Similarly, the ratio factor defined by Equation (21) can be expressed as:

$$Y_{ij}(C, T) = \frac{\sigma[\log V_i(t)]}{\sigma[\log V_j(t)]} \quad (32)$$

[0066] The mathematic correlation between optical measurement and blood glucose concentration can then be established according to Equation (22) or Equation (23), under corresponding calibration conditions. The schematic circuit diagram of a typical preamplifier **400** also includes a feedback capacitor **404**, an operational amplifier **406**, and a ground connection **410**.

Digitization

[0067] The voltage output **412** from the preamplifier **400** is usually digitized using an analog-to-digital convertor (ADC). The digitized signal is then sent to a computer for data analysis. The output of i th ADC, in communication with i th preamplifier that is in coupling with i th photodiode **408** collecting light power at wavelength A_{λ} , can be expressed by the following Equation:

$$(ADC)_i = (ADC)_{0i} + G \{ [I_D(\lambda_p, t) + I_{Dark,i}] R_i + A_{0i} \} \quad (33)$$

[0068] In the above Equation (33), $(ADC)_{0i}$ is the offset of i th ADC, G is the nominal ADC Gain used during the detection, $I_D(\lambda_p, t)$ is the photocurrent of i th photodiode detector, $I_{Dark,i}$ is the dark current of i th photodiode detector, $R_i = R_{0i} [1 + \gamma_{Ri}(T_{Ri}(t) - 25^\circ \text{C.})]$ is the resistance of feedback resistor of i th preamplifier, and A_{0i} is the offset of i th preamplifier.

[0069] The contribution of the three factors, $(ADC)_{0i}$, $I_{Dark,i}$, and A_{0i} can be removed by carrying out a dark measurement with the light source turned off right before or after the corresponding finger measurement. When the light source is turned off, the above Equation (33) becomes:

$$(ADC)_{Dark,i} = (ADC)_{0i} + G_i (I_{Dark,i} R_i + A_{0i}) \quad (34)$$

[0070] The difference between the two above Equations (33) and (34) reflects ADC output corresponding to the photocurrent:

$$\alpha(ADC)_i = (ADC)_i - (ADC)_{Dark,i} = G_i I_D(\lambda_p, t) R_i \quad (35)$$

[0071] Applying common logarithm to both side of the Equation (35), one obtains:

$$\log \Delta(ADC)_i = \log G_i + \log I_D(\lambda_p, t) + \log R_i \quad (36)$$

[0072] G_i and R_i can be considered as constants as long as the time interval between the finger measurement and the dark measurement is short. As such, one obtains:

$$\sigma[\log \Delta(ADC)_i] = \sigma[\log I_D(\lambda_p, t)] \quad (37)$$

Substituting Equation (26) into Equation (37), one further obtains:

$$\sigma[\log \Delta(ADC)_i] = \sigma[\log P(\lambda_p, t)] \quad (38)$$

[0073] Based on Equation (37), the normalization factor defined by Equation (18) can be expressed as:

$$Q_i(C, T) = \frac{\sigma[\log \Delta(ADC)_i]}{\sum_{i=1}^N \sigma[\log \Delta(ADC)_i]} \quad (39)$$

[0074] The mathematic correlation between optical measurement and blood glucose concentration can then be established according to Equation (19) or (20), under corresponding calibration conditions.

[0075] Similar to normalization, the ratio factor defined by Equation (21) can be expressed as:

$$Y_{ij}(C, T) = \frac{\sigma[\log \Delta(ADC)_i]}{\sigma[\log \Delta(ADC)_j]} \quad (40)$$

[0076] The correlation between optical measurement and blood glucose concentration can then be established according to Equations (22) or (23), under corresponding calibration conditions.

[0077] Thus, there has been shown and described several embodiments of a novel invention. As is evident from the foregoing description, certain aspects of the present invention are not limited by the particular details of the examples illustrated herein, and it is therefore contemplated that other modifications and applications, or equivalents thereof, will occur to those skilled in the art. The terms "have," "having," "includes," "including," and similar terms as used in the foregoing specification are used in the sense of "optional" or "may include" and not as "required." Many changes, modifications, variations and other uses and applications of the present construction will, however, become apparent to those skilled in the art after considering the specification and the accompanying drawings. All such changes, modifications, variations and other uses and applications, which do not depart from the spirit and scope of the invention, are deemed to be covered by the invention, which is limited only by the claims that follow. It should be understood that the embodiments disclosed herein include any and all combinations of features described in any of the dependent claims.

1-14. (canceled)

15. A system for detecting glucose in a biological sample, comprising:

- at least one light beam generating structure;
- at least one photocurrent signal generating light detector; and
- a light absorbance change determining algorithm implemented processor programmed to calculate a change in a light absorption caused by blood in a biological sample and configured to receive the output photocurrent signal from the at least one photocurrent signal

generating light detector and based on the received output photocurrent signal to determine a blood glucose level associated with the biological sample present in the target area.

16. The system of claim **15**, wherein the light absorbance change determining algorithm implemented processor is programmed to calculate the attenuance attributable to blood in the biological sample based on the received output photocurrent signal.

17. The system of claim **15**, wherein the light absorbance change determining algorithm implemented processor is programmed to eliminate effect of uncertainty caused by temperature dependent detector response of the at least one photocurrent signal generating light detector by calculating the standard deviation of a logarithm of the time dependent voltage signal.

18. The system of claim **15**, wherein the light absorbance change determining algorithm implemented processor is configured to calculate a normalization factor $Q_i(C, T)$ based on an output voltage $V_i(t)$ of the i^{th} preamplifier as a function of time, where σ is standard deviation according to the equation:

$$Q_i(C, T) = \frac{\sigma[\log V_i(t)]}{\sum_{i=1}^N \sigma[\log V_i(t)]};$$

wherein T is a temperature of the biological sample and C is the concentration of blood glucose in the biological sample.

19. The system of claim **15**, wherein the light absorbance change determining algorithm implemented processor is configured to calculate a ratio factor $Y_{ij}(C, T)$ based on an output voltage $V_i(t)$ of the preamplifier and an output voltage $V_j(t)$ of the j^{th} preamplifier as a function of time, where σ is standard deviation according to the equation:

$$Y_{ij}(C, T) = \frac{\sigma[\log V_i(t)]}{\sigma[\log V_j(t)]};$$

wherein T is a temperature of the biological sample and C is concentration of blood glucose in the biological sample.

20. The system of claim **15**, further comprising an analog-to-digital convertor having a digitized voltage output.

21. The system of claim **15**, wherein the light absorbance change determining algorithm implemented processor is configured to calculate a normalization factor $Q_i(C, T)$ based on a voltage output $\Delta(\text{ADC})_i$ of an i^{th} analog-to-digital converter, where σ is standard deviation according to the equation:

$$Q_i(C, T) = \frac{\sigma[\log \Delta(\text{ADC})_i]}{\sum_{i=1}^N \sigma[\log \Delta(\text{ADC})_i]}$$

wherein T is the temperature of the biological sample and C is the concentration of blood glucose in the biological sample.

22. The system of claim **15**, wherein the light absorbance change determining algorithm implemented processor is configured to calculate a ratio factor $Y_{ij}(C, T)$ based on a voltage output $\Delta(\text{ADC})_i$ of the i^{th} analog-to-digital convertor and a voltage output $\Delta(\text{ADC})_j$ of the j^{th} analog-to-digital convertor, where σ is standard deviation according to the equation:

$$Y_{ij}(C, T) = \frac{\sigma[\log \Delta(\text{ADC})_i]}{\sigma[\log \Delta(\text{ADC})_j]}$$

wherein T is a temperature of the biological sample and C is a concentration of blood glucose in the biological sample.

23. The system of claim **15**, wherein the at least one light beam generating structure is configured to strike a target area of a biological sample and generates one or more light beams having a wavelength in a range between 800 nm and 1600 nm.

24. The system of claim **15**, wherein the at least one photocurrent signal generating light detector includes a preamplifier having a feedback resistor, positioned to receive light from the at least one light source and to generate an output photocurrent signal, having a time dependent current, which is indicative of the power of light detected.

25. The system of claim **24**, wherein the preamplifier has a feedback resistor, which is configured to convert the time dependent current into a time dependent voltage signal.

26. A method for detecting glucose in a biological sample, comprising:

utilizing at least one light beam generating structure to generate one or more light beams to strike a target area of a biological sample;

utilizing at least one photocurrent signal generating light detector; and

receiving an output photocurrent signal from the at least one photocurrent signal generating light detector with a light absorbance change determining algorithm implemented processor programmed to calculate a change in a light absorption caused by blood in the biological sample and based on the received output photocurrent signal to determine a blood glucose level associated with the biological sample present in the target area based on the calculated attenuance with the light absorbance change determining algorithm implemented processor.

27. The method of claim **26**, wherein the one or more light beams have a wavelength in a range between 800 nm and 1600 nm.

28. The method of claim **26**, further comprising a preamplifier having a feedback resistor, positioned to receive light from the at least one light source and generating an output photocurrent signal, having a time dependent current, which is indicative of the power of light detected.

29. The method of claim **28**, further comprising converting the time dependent current into a time dependent voltage signal.

30. The method of claim **26**, further comprising calculating attenuance attributable to blood in the biological sample present in the target area by using the light absorbance change determining algorithm implemented processor.

31. The method of claim **26**, further comprising calculating a normalization factor $Q_i(C, T)$ based on the voltage output $V_i(t)$ of the i^{th} preamplifier as a function of time, where σ is standard deviation according to the equation:

$$Q_i(C, T) = \frac{\sigma[\log V_i(t)]}{\sum_{i=1}^N \sigma[\log V_i(t)]};$$

wherein T is a temperature of the biological sample and C is a concentration of blood glucose in the biological sample.

32. The method of claim **26**, further comprising calculating a ratio factor $Y_{ij}(C, T)$ based on an output voltage $V_i(t)$ of the i^{th} preamplifier and an output voltage $V_j(t)$ of the j^{th} preamplifier as a function of time, where σ is standard deviation according to the equation:

$$Y_{ij}(C, T) = \frac{\sigma[\log V_i(t)]}{\sigma[\log V_j(t)]};$$

wherein T is a temperature of the biological sample and C is a concentration of blood glucose in the biological sample.

33. The method of claim **26**, further comprising utilizing an analog-to-digital convertor having a digitized voltage output.

34. The method of claim **26**, further comprising calculating a normalization factor $Q_i(C, T)$ based on a voltage output $\Delta(ADC)_i$ of an i^{th} analog-to-digital convertor, where σ is standard deviation according to the equation:

$$Q_i(C, T) = \frac{\sigma[\log \Delta(ADC)_i]}{\sum_{i=1}^N \sigma[\log \Delta(ADC)_i]}$$

wherein T is a temperature of the biological sample and C is a concentration of blood glucose in the biological sample.

35. The method of claim **26**, further comprising calculating a ratio factor $Y_{ij}(C, T)$ based on a voltage output $\Delta(ADC)_i$ of an i^{th} analog-to-digital convertor and a voltage output $\Delta(ADC)_j$ of a j^{th} analog-to-digital convertor, where σ is standard deviation according to the equation:

$$Y_{ij}(C, T) = \frac{\sigma[\log \Delta(ADC)_i]}{\sigma[\log \Delta(ADC)_j]}$$

wherein T is a temperature of the biological sample and C is a concentration of blood glucose in the biological sample.

36. A system for detecting glucose in a biological sample, comprising:

at least one light beam generating structure;

at least one photocurrent signal generating light detector; and

a light absorbance change determining algorithm implemented processor programmed to calculate a change in a light absorption caused by blood in a biological sample and configured to receive the output photocurrent signal from the at least one photocurrent signal generating light detector and based on the received output photocurrent signal to determine a blood glucose level associated with the biological sample present in the target area, wherein the light absorbance change determining algorithm implemented processor is programmed to eliminate effect of uncertainty caused by temperature dependent detector response of the at least one photocurrent signal generating light detector.

* * * * *

专利名称(译)	利用光谱数据分析进行非侵入式光学血糖检测的方法和系统		
公开(公告)号	US20180055425A1	公开(公告)日	2018-03-01
申请号	US15/806242	申请日	2017-11-07
[标]申请(专利权)人(译)	圣路易斯医疗器械公司		
申请(专利权)人(译)	圣路易斯医疗器械公司		
当前申请(专利权)人(译)	圣路易斯医疗器械公司		
[标]发明人	XU ZHI		
发明人	XU, ZHI		
IPC分类号	A61B5/145 A61B5/1455 A61B5/00		
CPC分类号	A61B5/1455 A61B2562/0238 A61B5/6838 A61B5/7225 A61B5/6826 A61B5/14532 A61B2576/00 G06F19/00		
优先权	61/055303 2008-05-22 US 61/089152 2008-08-15 US		
外部链接	Espacenet USPTO		

摘要(译)

公开了用于基于光谱数据非侵入地测量生物样品中的血糖水平的系统和方法。这包括至少一个被配置为撞击样本的目标区域的光源，至少一个光检测器，其包括具有反馈电阻器的前置放大器，被定位成接收来自至少一个光源的光并产生输出信号，具有时间相关的电流，其指示检测到的光的功率，并且处理器被配置为从所述至少一个光检测器接收输出信号并且基于所接收的输出信号，计算可归因于存在的样本中的血液的衰减。在目标区域中并且消除由至少一个光检测器的温度依赖性检测器响应引起的不确定性的影响，并且基于所计算的衰减，确定与样本相关联的血糖水平。

